AQUA
Water Infrastructure, Ecosystems and Society

IWA PUBLISHING

 AQUA — Water Infrastructure, Ecosystems and Society Vol 70 No 6, 811 doi: 10.2166/aqua.2021.050

Structural property and risk assessment of loose deposits in drinking water distribution systems

Yuan Zhuang[a], Xinyi Qin[a], Yongtong Li[a], Shuo Xu[a], Ying Yu[a], Yifan Gu[b] and Baoyou Shi[a,c,*]
[a] Key Laboratory of Drinking Water Science and Technology, Research Center for Eco-Environmental Sciences, Chinese Academy of Sciences, Beijing 100085, China
[b] State Key Laboratory of Pollution Control and Resource Reuse, School of Environmental Science and Engineering, Tongji University, Shanghai 200092, China
[c] University of Chinese Academy of Sciences, Beijing 100049, China
*Corresponding author. E-mail: byshi@rcees.ac.cn

BS, 0000-0003-2129-4717

ABSTRACT

Discoloration events caused by loose deposits resuspension in drinking water distribution systems (DWDS) are the main aspects of customer complaints across the world, but the understanding of the potential risks of loose deposits is insufficient. In this study, loose deposits in real DWDS were collected from regions frequently experiencing 'yellow water'. Cytotoxicity of healthy human liver cells was used to evaluate the toxicity risks of the particle samples. The results showed that the loose deposits would have a realistic discoloration risk (turbidity $>$ 10 NTU) when their concentrations were higher than 10 mg/L. The water sample containing 1,000 mg/L loose deposits had a dark yellow color (100–300 PCU) and cytotoxicity (viability of human liver cells during cytotoxicity tests 59.18–80.69%), while the water sample containing 1 mg/L loose deposits did not have obvious color ($<$15 PCU) and cytotoxicity ($>$97.00%). Particle size showed a stronger correlation with relative viability ($r = 0.761$) than other properties (specific area, metal content, contact angle, saturation magnetization and electron transfer number). However, it is interesting to note that both turbidity and color had a low correlation with relative viability, thus the toxicity of the particles could not be properly judged using turbidity or color. This study gives an important guidance that although the loose deposits could be visualized during water discoloration, its toxicity risks could not be evaluated through aesthetic indicators.

Key words: discoloration events, drinking water distribution system, loose deposits

HIGHLIGHTS

- Loose deposits $>$10 mg/L had a realistic discoloration risk.
- The cell viability of 1,000 mg/L loose deposit particles was 59.18–80.69%.
- Particle size showed a stronger correlation with toxicity than other properties.
- Toxicity of loose deposits could not be judged using turbidity or color.

GRAPHICAL ABSTRACT

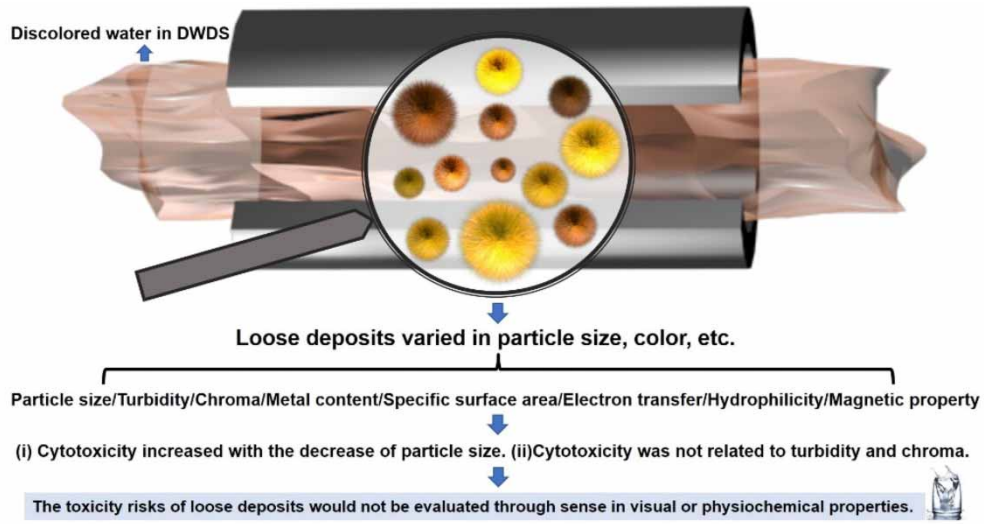

1. INTRODUCTION

Although treatment processes at plants could significantly improve water quality, finished water entering into a drinking water distribution system (DWDS) usually includes particles, microbial loads and nutrients (Liu *et al.* 2013). While traveling in a DWDS, the above-mentioned particles can be transported by the water flow throughout the network or be deposited as loose deposits depending on their characteristics and the flow conditions (Vreeburg & Boxall 2007; Liu *et al.* 2014). In a DWDS, there are complex origins for loose deposits formation, including residual matter from raw water (residual particles and residual metallic elements, such as iron) and corrosion products from pipes. Internal corrosion inevitably happens in DWDS due to the interaction between water and pipe material (Zhang *et al.* 2020a). Notably, once a disturbance has occurred, loose deposits would resuspend to induce water quality deterioration, such as an increase of turbidity and discoloration. Discoloration events caused by particle resuspension are the main aspects of complaints related to drinking water worldwide which have drawn extensive attention from both the societal communities and scientific arena (Vreeburg & Boxall 2007). Particles in discolored water could be exposed to living beings through drinking water or other ways using water. The potential harmful effects of small particles depend on their physicochemical properties. The particles with smaller sizes may favor their entry into the cells and eventually lead to stronger cytotoxic and genotoxic effects than larger particles (Cronholm *et al.* 2013).

However, discoloration events resulting from loose deposits are usually considered as aesthetic issues rather than health risks. Furthermore, particle properties and their relationship with particle toxicity are unclear. Gerke *et al.* (2008) found that although water quality could affect the physiochemical properties of iron tubercles, it was not the main controlling factor. Boxall & Saul (2005) found that the distribution of particle sizes in discolored water was repeatable and independent of DWDS conditions, while the size range was primarily smaller than 50 μm with an average of about 10 μm. Commonly, the toxicity of particles increases with decreasing size (Suresh *et al.* 2013). The toxicity of particles especially in nanoscale has been investigated for more than a decade. As the size range of the loose deposits in a DWDS is similar in different systems, the size may be a useful indicator of the toxicity of loose deposits in a DWDS. Besides size, the shape could also affect toxicity. As heavy metals contained in the loose deposits in a DWDS possess toxicity, there have been investigations that indirectly indicate the toxicity of the loose deposits in a DWDS using the metal content, but the toxicity of these particles has not been confirmed using toxicity tests (Liu *et al.* 2015, 2018). Liver uptake is the most effective elimination pathway of iron oxide nanoparticles (Briley-Saebo *et al.* 2011), and Zhuang *et al.* (2019, 2021) found that FeOOH particles, which are one of the most representative components of loose deposits in DWDS, could have different morphologies under different coexistence conditions, resulting in differences in their cytotoxicity to healthy human liver cells. However, in a common sense, the complaint degree on discoloration is mainly based on the color or turbidity of drinking water. Thus, people may deduce the toxicity risks of the discolored drinking water based on their visual sense. The safety of drinking water is

important, but the toxicity effect of loose deposits in DWDS has not been extensively recognized. However, which factor (including particle size, particle shape, turbidity and color) could reflect the potential risks of real loose deposits in a DWDS is still unclear.

Accurate assessment of cytotoxicity is a critical prerequisite in toxicity studies. It is well known that the reduction of particle size from macroscopic to nanometer scale, the chemical and physical properties may change due to the size and surface effects. In bulk materials, the ratio of surface atoms to that of interior atoms is small and the surface effect is insignificant. This ratio noticeably increases with decreasing particle size and, the surface effect may dominate the material properties (Yin *et al.* 2005). According to the traditional law of toxicity, particle size is a useful indicator. However, real loose deposits in DWDS are a mixture of complex components, including various crystals and amorphous structures, and whether the size rule is useful under this condition should be confirmed. Moreover, although the components of particles are very different among different DWDS conditions, the properties possessed by whole particles may be in a similar range, such as the specific area, which could affect the accumulation effect of particles (Zhuang *et al.* 2020). Thus, different physicochemical properties and electrochemical properties should also be considered.

In this study, loose deposits in a real DWDS were collected from the DWDS in regions that have frequently experienced 'yellow water'. Then, physicochemical property, electrochemical property and cytotoxicity of the loose deposits were characterized. The turbidity and color of the water containing different concentration of loose deposits were tested. The relationship among these characteristics was analyzed to reveal the factor that might determine the potential risks of loose deposits in a DWDS.

2. MATERIALS AND METHODS

2.1. Sampling process

We sampled 12 different DWDS sites to collect loose deposits in a metropolitan city in northern China. These sites contained mainly old unlined cast iron pipes with relatively high pipe ages (15–20 years old or more) where discoloration was frequently experienced. To collect loose deposits, the hydrant was turned on at the selected sampling location with custom mesh covered on the discharge stream under flushing flow velocity (20 L/s). The synthetic nylon mesh net was 380 mm in length, 50 μm in pore size and 105 mm in diameter. The hydrant was turned on fully for about 6 min to get deposits (Liu *et al.* 2018). After discharging, the net was removed from the hydrants and taken back to the laboratory immediately. The loose deposits were freeze-dried for 18 h. After drying, to make the samples more uniform, the loose deposits were crushed and sieved using a No. 90 sieve (160-μm mesh). These loose deposits were numbered as sample 1# to 12#. The loose deposit solution was obtained by dispersing loose deposits into distilled water resulting in concentrations of 0.01–1,000 mg/L.

2.2. Characterization of loose deposits

Microscopy images of the samples were taken by microscopy (Leica MGD41). The morphologies of all the loose deposits were characterized using field-emission scanning electron microscopy (SEM, Hitachi S4800). Turbidity of the loose deposit solution was tested by a turbidimeter (Hach 2100Q) immediately after the sample was shaken for 5 min. Color of the loose deposit solution was measured by the Pt–Co method unit. The zeta potential and particle size of the loose deposits were determined in solution using a zeta potential analyzer (Malvern, Zetasizer2000). To get the specific surface area and pore distributions, the loose deposits were degassed at 373 K for 6 h and measured through the nitrogen adsorption/desorption method using an accelerated surface area and porosimetry system (Micromeritics, ASAP 2020) at 77.4 K. The contact angle was measured using a contact angle tester (OCA 20, DataPhysics). Magnetic measurements were operated using a vibrating sample magnetometer (VSM). Cyclic voltammetry (CV) tests of various samples were performed using a basic electrochemical system (CHI, 760E). All the tests were operated in a three-electrode system using 1 M KCl-Ag/AgCl as the reference electrode, Pt wire as the counter electrode and a glassy carbon (GC) electrode as the working electrode. CV curves were carried out at a scan rate of 10 mV/s in Ar- and O_2-saturated 0.1 M KOH solution for the ORR. Rotating disk electrode (RDE) experiments were operated on an RRDE-3A (Ver 2.0) in O_2-saturated 0.1 M KOH solution at a scan rate of 10 mV/s.

2.3. Toxicity evaluation

To evaluate the toxicity of the loose deposits, nonradioactive and colorimetric 3-(4,5-dimethylthiazol-2-yl)-2,5-diphenyltetrazolium bromide (MTT) assay was used (Pieters *et al.* 1989). Dimethyl sulfoxide (DMSO) was used to dissolve cell membranes

with absorbance at 570 nm on a microplate reader (EPOCH2T, Biotek) to reflect the quantity of living cells. We used healthy human liver cells from the Shanghai Cell Bank of the Chinese Academy of Sciences. The cells were cultured in an incubator at 37 °C under the atmosphere of 5% CO_2. The materials were sterilized by ultraviolet irradiation for 30 min before being used to logarithmically count and collect the LO_2 cells. Then, 100 μL of cell suspension was added to the well plate at a rate of 2×10^4 cells/well. The control experiment was conducted with no addition of loose deposits. The culture medium was removed after different times (24, 48, 72, 120 and 168 h). The medium was removed after incubation followed by the formazan crystals solubilized with 150 μL isopropanol in an incubator. The viability was a mean value of 3 duplicate experiments. If cells are 100% viable, there is no toxicity of the particle solution, but if the percentage viable cells decrease, the toxicity increases.

3. RESULTS AND DISCUSSION

3.1. Appearance, microstructure and toxicity

Particles were dispersed into distilled water with a series of concentrations, as shown in Figure 1 (500 mg/L with color similar to the real 'yellow water') and Figure S1 (Supplementary Information). At 1,000 mg/L, all the solutions had a dark yellow color. When the concentration was below 100 mg/L, it was difficult to observe the color with the naked eye. At 500 mg/L, the solutions had distinguishable color, with 5# being the darkest and 7# being the lightest in visual. SEM images of the samples are shown in Figure 2. Most of the samples had sea urchin-like structures with abundant stabs. In the microscopy images of the samples (Figure S2), most of the thick particles were a dark gray color, which may mainly contain stable iron oxides such as Fe_3O_4, but some of the thin parts were an obvious orange color, which may mainly contain unstable iron oxides such as FeOOH. Thus, the chromogenic substance in loose deposits in 'yellow water' events would mainly be the new generated iron oxides. The turbidity and color of the particle solutions at different concentrations are shown in Figures 3 and 4. Sample #8 had the highest turbidity, while sample 3# had the highest color. When the particle concentration was lower than 1 mg/L, the turbidity of all samples was below 10 NTU, and the color values of all samples were all below 15; when the particle concentration was 10 mg/L, the turbidity of some samples (samples 7# and 8#) was higher than 10 NTU. As the visibility turbidity threshold is 10 NTU (Vreeburg *et al.* 2008), a particle concentration higher than 10 mg/L would have a realistic discoloration risk.

The diet of water is accompanied by particle intake, resulting in health risks, with liver uptake as the most effective method of conversion (Briley-Saebo *et al.* 2011). Hence, we chose healthy human liver cells to evaluate particle toxicity. In the florescence microscopy images, green cells were alive, while red cells were dead (Figure 5(a)). The toxicity results of the

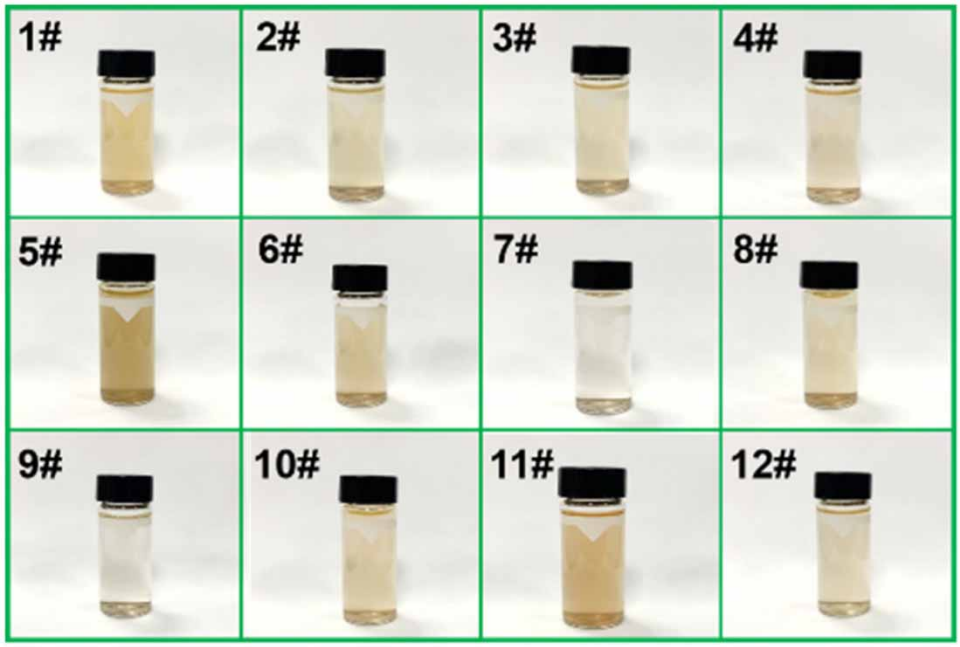

Figure 1 | Photographs of the particle solutions at 500 mg/L.

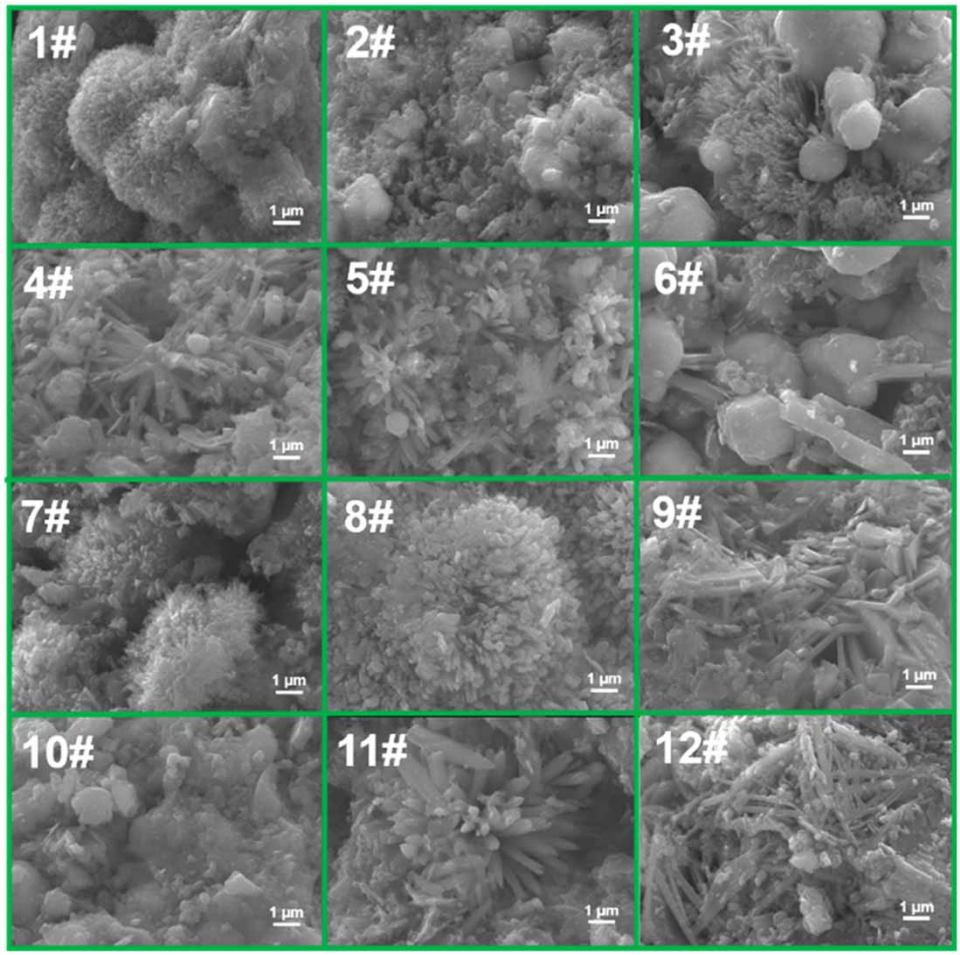

Figure 2 | SEM images of the particle samples.

MTT assay results are shown in Figure 5(b). At a particle concentration of 1,000 mg/L, which could be sensed as obvious 'yellow water', the cell viability ranged from 59.18% (sample #10) to 80.69% (sample 7#). Discoloration problems in a DWDS are commonly considered aesthetic issues rather than health risks (Sun *et al.* 2017). In addition, complaints about 'yellow water' were usually judged by the naked eye. However, it is very interesting to note that sample #5, which seemed darkest in visual, did not have the highest toxicity, thereby providing very important enlightenment that we could not evaluate the harmful effects of discolored water based only on colors. When the particle concentration was below 1 mg/L, the cell viability of all samples was higher than 97.00%. Thus, the samples with obvious color had obvious toxicity, but samples without an obvious color were hard to predict. Therefore, it should be noted that discolored water without an obvious color may also have certain toxicity.

3.2. Particle structure analysis

Particle size influences many properties of particulate materials (e.g. stability and reactivity) (Freitas *et al.* 2020). The average size of the particles in the DWDS was found to be repeatable and independent from DWDS conditions (10 μm) (Boxall & Saul 2005); however, particles that present toxicity are usually at the nanoscale. Thus, we tested particles in the DWDS with an average particle size below 10 μm (Table 1). In addition to particle size, previous literature has used the heavy metal content, which indirectly indicates the toxicity of particles in a DWDS (Liu *et al.* 2015, 2018). For example, Al intake from drinking water could induce kidney nerve damage and disorder (Tian *et al.* 2020). Particles in DWDSs commonly contain various heavy metals, such as Fe, Mn, Al, Zn, Pb, Cu, Cr and Cd, among which Fe is the primary metal element (Liu *et al.* 2016). Han *et al.* (2018) found an obvious positive correlation between Fe and other heavy metals, such as As, in loose

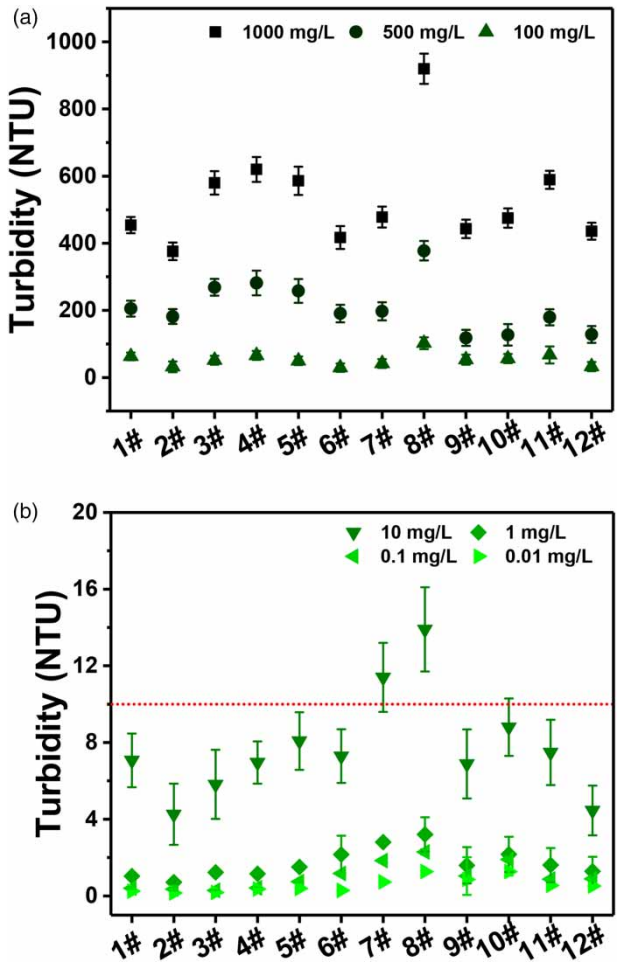

Figure 3 | Turbidity of the particle solutions in a series of concentrations (a) 1,000, 500 and 100 mg/L, (b) 10, 1, 0.1 and 0.01 mg/L (the red line is the visibility turbidity threshold).

deposits. Thus, the Fe content may reflect the heavy metal content in loose deposits. Here, among the various metals in the loose deposits, Fe had the highest content in the particles (Figure S3). In addition to Fe, there was also an abundance of Ca, Mg, Si, Cu and Cr in these samples. The Mn in these samples was below 10 g/kg, indicating that Fe was the coloring element in these samples. All the samples were hydrophilic (Figure S4), with contact angles between 18.25° (sample 7#) and 42.74° (sample 10#). The N_2 adsorption–desorption isotherms and the corresponding BJH pore size distributions are shown in Figure S5, while the BET specific surface area, pore diameter and pore volume of the samples are shown in Table 2. The sample with the highest specific area was sample 7# (54.2 m^2/g), while the lowest was sample 5# (16.8 m^2/g). Zhang *et al.* (2020b) found that magnetic iron oxides would enhance the toxicity effect because it enhances the co-deposition of other ferromagnetic or paramagnetic substances and promotes the accumulation in the human body. The magnetization curves and saturation magnetization values of the particles are shown in Figure S6a and S6b. Samples 1# to 12# all had good magnetic properties. Sample 7# had the lowest saturation magnetization value among these samples.

Iron species in loose deposits have been found to be able to not only capture electrons from oxygen to generate free radicals but also get electrons directly from cells to cause oxidative damage (Zhuang *et al.* 2019), thus the electrochemical performances of the loose deposits were also taken into consideration. The electrocatalytic activity of the materials was examined by studying the redox reactions using CV (Figure S7), which showed that the reduction peaks of most of these samples were at approximately −0.9 V. RDE voltammograms at different rotation rates are shown in Figure S8. The corrosion current densities of the samples are shown in Figure S10, indicating that sample 7# had the highest potential for corrosion. Based on Tafel plots (Figure S9) and Koutecky–Levich plots at different electrode potentials (Figure S10), the number of electrons

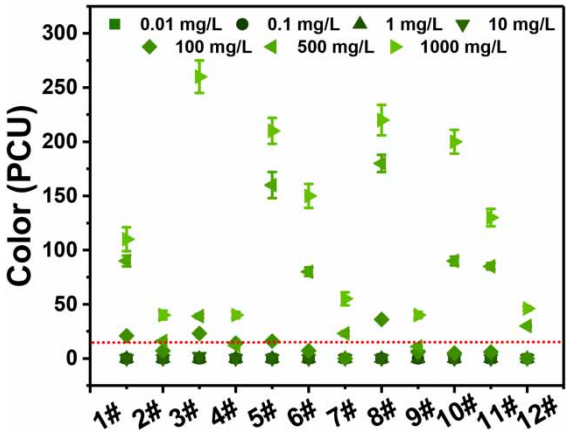

Figure 4 | Color of the particle solutions in a series of concentrations (the red line is the standard color limits in China GB5749-2006).

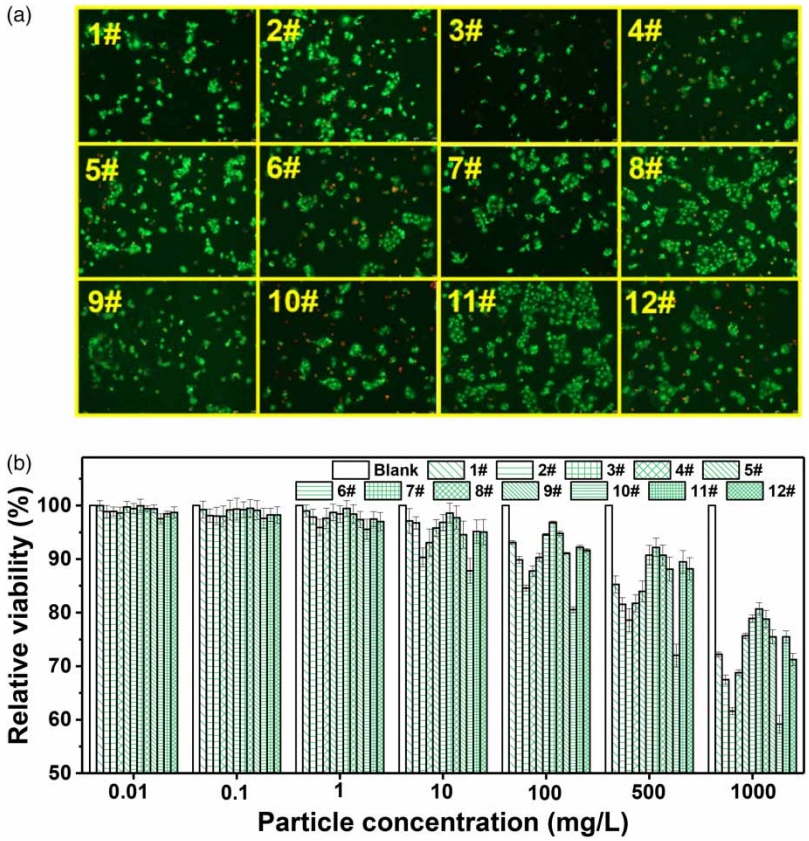

Figure 5 | (a) Fluorescence microscopy images of cells treated with 10 mg/L particles (green: live cells, red: dead cells) and (b) relative viabilities, as determined via MTT assay of the particles.

transferred (Figure S11) can be obtained. The linearity and parallelism of the Koutecky–Levich plots are recognized as first-order reaction kinetics in regard to the dissolved oxygen concentration. The electron transfer number varies between 0 and 4 and is dependent on the overpotential. Most of the samples followed a 4-electron transfer pathway in ORR. The increase of electron transfer number around −0.3 V indicated other redox reactions happened during ORR, which was in accordance with the inevitable free radical generation with the iron species as electron acceptor in previous literature (Zhuang *et al.* 2019).

Table 1 | Average size and zeta potential of the samples

Sample	Average size (nm)	Zeta potential (mV)
1#	1,886	2.33
2#	1,133	4.26
3#	1,068	5.16
4#	1,433	−1.63
5#	1,532	−6.46
6#	2,853	3.94
7#	5,116	−1.94
8#	4,549	6.55
9#	1,165	3.46
10#	400.5	2.58
11#	1,911	9.13
12#	1,842	−5.46

Table 2 | BET specific surface area, pore volume and pore diameter of the samples

Sample	Specific area (m^2/g)	Pore diameter (nm)	Pore volume (cm^3/g)
1#	43.6	6.69	0.073
2#	29.7	6.78	0.051
3#	35.7	6.40	0.057
4#	24.3	5.96	0.036
5#	16.8	20.26	0.086
6#	29.8	8.32	0.062
7#	54.2	5.60	0.076
8#	50.0	11.07	0.139
9#	46.7	7.33	0.086
10#	37.6	5.56	0.052
11#	32.1	8.92	0.071
12#	26.6	6.42	0.042

3.3. Relevance between toxicity and structural properties of the loose deposits

In the result of principal component analysis (Figure 6 and Table 3), relative viability and particle size showed the strongest correlation ($r = 0.761$), which was much stronger than other properties (specific area, metal content, contact angle, saturation magnetization and electron transfer number). Here, particles with smaller size had higher toxicity, the reason for which may be that particles with smaller size have a higher ability to cause oxidative stress response with the generation of reactive oxygen species (ROS) (Park *et al.* 2011). The ROS include the singlet oxygen, the extremely reactive superoxide anion radical, associated with the activation of apoptosis and hydrogen peroxide, which can be reduced partially to the reactive hydroxyl radical, which in turn can attack and damage DNA and proteins. Intracellular ROS can also induce lipid peroxidation and protein oxidation. ROS can also originate at the particles' surface, owing to their semiconductor and electronic properties (Santos *et al.* 2010). Particles with smaller size contact with each cell easier than those with larger size to generate cytotoxicity (Santos *et al.* 2010). Although referred to as discoloration, it is difficult for customers to visually observe discoloration and accurately correlate it to water quality. Therefore, turbidity is the measurable parameter. However, the effects on the perceived turbidity or discoloration caused by different particles have significant differences (Vreeburg & Boxall 2007). For these

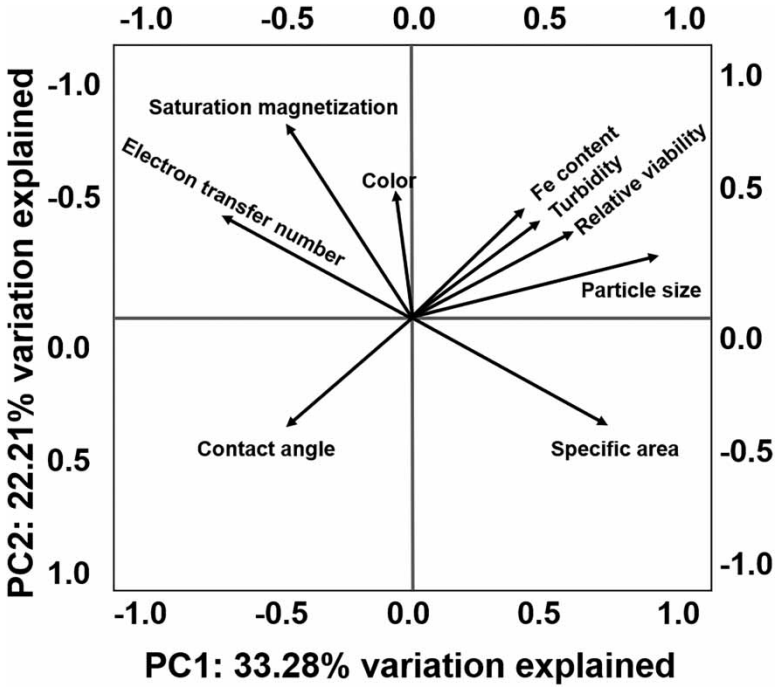

Figure 6 | Principal component analysis (PCA) of toxicity and structural properties of the loose deposits.

Table 3 | PCA general approach: correlations matrix variables

	a	b	c	d	e	f	g	h	i
a	1	0.199	−0.220	0.265	0.149	−0.284	0.252	−0.183	**0.761****
b	0.199	1	0.508	0.174	0.140	−0.173	0.064	−0.362	0.404
c	−0.220	0.508	1	−0.058	0.343	0.137	0.264	0.185	−0.030
d	0.265	0.174	−0.058	1	0.113	0.068	−0.664*	−0.483	0.560
e	0.149	0.140	0.343	0.113	1	−0.429	−0.022	−0.128	0.356
f	−0.284	−0.173	0.137	0.068	−0.429	1	−0.039	0.107	−0.522
g	0.252	0.064	0.264	−0.664*	−0.022	−0.039	1	0.672*	−0.168
h	−0.183	−0.362	0.185	−0.483	−0.128	0.107	0.672*	1	−0.407
i	**0.761****	0.404	−0.030	0.560	0.356	−0.522	−0.168	−0.407	1

a: relative viability, b: turbidity, c: color, d: specific area, e: Fe content, f: contact angle, g: saturation magnetization, h: electron transfer number, i: particle size.
*Correlation is significant at the 0.05 level.
**Correlation is significant at the 0.01 level.

samples, turbidity and color had a certain positive correlation ($r = 0.508$). However, both turbidity and color had a low correlation with relative viability ($r = 0.199, -0.220$), thus the toxicity of the particles could not be properly judged using turbidity or color.

4. CONCLUSION

Drinking water discoloration events caused by loose deposits in DWDS are important aspects of customer complaints on water quality, but the structural property and toxicity of the loose deposits were not clear. Herein, we collected loose deposits in a real DWDS from regions that frequently experience 'yellow water'. The results showed that particle concentrations higher than 10 mg/L (turbidity > 10 NTU) would have a realistic discoloration risk. The cell viabilities of healthy human liver cells

ranged from 59.18 to 80.69% under dark yellow water conditions in this toxicity test. When the particle concentration was below 10 mg/L with no obvious color, the cell viability of all the samples was higher than 97.00%. Relative viability and particle size showed the strongest correlation ($r = 0.761$) compared to other properties (specific area, metal content, contact angle, saturation magnetization and electron transfer number). However, it is interesting to notice that both turbidity and color had a low correlation with relative viability, thus the toxicity of the particles could not be properly judged using turbidity or color. This study gives important guidance that though discoloration events caused by loose deposits are usually considered as aesthetic problems, its toxicity risks could not be evaluated through visual appearance.

ACKNOWLEDGEMENTS

This research was supported by the National Key R&D program of China (2018YFE0204103) and the National Natural Science Foundation of China (Nos. 51808538, 51978652).

DATA AVAILABILITY STATEMENT

All relevant data are included in the paper or its Supplementary Information.

REFERENCES

Boxall, J. B. & Saul, A. J. 2005 Modeling discoloration in potable water distribution systems. *J. Environ. Eng.* **131**, 716–725.

Briley-Saebo, K. C., Cho, Y. S., Shaw, P. X., Ryu, S. K., Mani, V., Dickson, S., Izadmehr, E., Green, S., Fayad, Z. A. & Tsimikas, S. 2011 Targeted iron oxide particles for in vivo magnetic resonance detection of atherosclerotic lesions with antibodies directed to oxidation-specific epitopes. *J. Am. Coll. Cardiol.* **57**, 337–347.

Cronholm, P., Karlsson, H. L., Hedberg, J., Lowe, T. A., Winnberg, L., Elihn, K., Wallinder, I. O. & Möller, L. 2013 Intracellular uptake and toxicity of Ag and CuO nanoparticles: a comparison between nanoparticles and their corresponding metal ions. *Small* **9**, 970–982.

Freitas, F. M. C., Cerqueira, M. A., Gonçalves, C., Azinheiro, S., Garrido-Maestu, A., Vicente, A. A., Pastrana, L. M., Teixeira, J. A. & Michelin, M. 2020 Green synthesis of lignin nano- and micro-particles: physicochemical characterization, bioactive properties and cytotoxicity assessment. *Int. J. Biol. Macromol.* **163**, 1798–1809.

Gerke, T. L., Maynard, J. B., Schock, M. R. & Lytle, D. L. 2008 Physiochemical characterization of five iron tubercles from a single drinking water distribution system: possible new insights on their formation and growth. *Corros. Sci.* **50**, 2030–2039.

Han, B., Chen, R., Shi, B., Xu, W. & Zhuang, Y. 2018 Practical evaluation of inorganic contaminant presence in a drinking water distribution system after hydraulic disturbance. *Journal of Water Supply: Research and Technology – AQUA* **67**, 12–21.

Liu, G., Verberk, J. Q. J. C. & Van Dijk, J. C. 2013 Bacteriology of drinking water distribution systems: an integral and multidimensional review. *Appl. Microbiol. Biotechnol.* **97**, 9265–9276.

Liu, G., Bakker, G. L., Li, S., Vreeburg, J. H. G., Verberk, J. Q. J. C., Medema, G. J., Liu, W. T. & Van Dijk, J. C. 2014 Pyrosequencing reveals bacterial communities in unchlorinated drinking water distribution system: an integral study of bulk water, suspended solids, loose deposits, and pipe wall biofilm. *Environ. Sci. Technol.* **48**, 5467–5476.

Liu, J., Chen, H., Huang, Q., Lou, L., Hu, B., Endalkachew, S.-D., Mallikarjuna, N., Shan, Y. & Zhou, X. 2015 Characteristics of pipe-scale in the pipes of an urban drinking water distribution system in eastern China. *Water Supply* **16**, 715–726.

Liu, J., Chen, H., Yao, L., Wei, Z., Lou, L., Shan, Y., Endalkachew, S.-D., Mallikarjuna, N., Hu, B. & Zhou, X. 2016 The spatial distribution of pollutants in pipe-scale of large-diameter pipelines in a drinking water distribution system. *J. Hazard Mater.* **317**, 27–35.

Liu, Q. L., Han, W. Q., Han, B. J., Shu, M. & Shi, B. Y. 2018 Assessment of heavy metals in loose deposits in drinking water distribution system. *Environ. Monit. Assess.* **190**, 388.

Park, J., Lim, D. H., Lim, H. J., Kwon, T., Choi, J. S., Jeong, S., Choi, I. H. & Cheon, J. 2011 Size dependent macrophage responses and toxicological effects of Ag nanoparticles. *Chem. Commun.* **47**, 4382–4384.

Pieters, R., Huismans, D. R., Leyva, A. & Veerman, A. J. P. 1989 Comparison of the rapid automated Mtt-assay with a dye exclusion assay for chemosensitivity testing in childhood leukemia. *Brit. J. Cancer* **59**, 217–220.

Santos, H. A., Riikonen, J., Salonen, J., Mäkilä, E., Heikkilä, T., Laaksonen, T., Peltonen, L., Lehto, V.-P. & Hirvonen, J. 2010 In vitro cytotoxicity of porous silicon microparticles: effect of the particle concentration, surface chemistry and size. *Acta Biomater.* **6**, 2721–2731.

Sun, H. F., Shi, B. Y., Yang, F. & Wang, D. S. 2017 Effects of sulfate on heavy metal release from iron corrosion scales in drinking water distribution system. *Water Res.* **114**, 69–77.

Suresh, A. K., Pelletier, D. A. & Doktycz, M. J. 2013 Relating nanomaterial properties and microbial toxicity. *Nanoscale* **5**, 463–474.

Tian, C., Feng, C., Chen, L. & Wang, Q. 2020 Impact of water source mixture and population changes on the Al residue in megalopolitan drinking water. *Water Res.* **186**, 116335.

Vreeburg, J. H. G. & Boxall, J. B. 2007 Discolouration in potable water distribution systems: a review. *Water Res.* **41**, 519–529.

Vreeburg, J. H. G., Schippers, D., Verberk, J. Q. J. C. & van Dijk, J. C. 2008 Impact of particles on sediment accumulation in a drinking water distribution system. *Water Res.* **42**, 4233–4242.

Yin, H., Too, H. P. & Chow, G. M. 2005 The effects of particle size and surface coating on the cytotoxicity of nickel ferrite. *Biomaterials* **26**, 5818–5826.

Zhang, H., Zhao, L., Liu, D., Wang, J., Zhang, X. & Chen, C. 2020a Early period corrosion and scaling characteristics of ductile iron pipe for ground water supply with sodium hypochlorite disinfection. *Water Res.* **176**, 115742.

Zhang, Q., Lu, D., Wang, D., Yang, X., Zuo, P., Yang, H., Fu, Q., Liu, Q. & Jiang, G. 2020b Separation and tracing of anthropogenic magnetite nanoparticles in the urban atmosphere. *Environ. Sci. Technol.* **54**, 9274–9284.

Zhuang, Y., Han, B., Chen, R. & Shi, B. 2019 Structural transformation and potential toxicity of iron-based deposits in drinking water distribution systems. *Water Res.* **165**, 114999.

Zhuang, Y., Han, B., Chen, R. & Shi, B. 2020 Mechanism study on organic pollutant accumulation by iron-based particles in drinking water conditions. *Chem. Eng. J.* **396**, 125157.

Zhuang, Y., Shen, C., Gu, Y., Chen, R. & Shi, B. 2021 Effect of trichloroacetic acid on iron oxidation: implications on the control of DBPs and deposits in drinking water. *Water Res.* **189**, 116632.

First received 13 April 2021; accepted in revised form 21 June 2021. Available online 7 July 2021